Nanomaterials and Nanocatalysis: An Interdependence Concept

Gurpreet Kour [a]

[a]Department of Chemistry, University of Jammu, India,180006.

Abstract

The present manuscript discusses an interdependence of a wider approach of nanomaterials synthesis to a relatively narrower energy concept called nanocatalysis. There are many different types of nanomaterials depending upon their composition and nature which can be used to study catalysis for different conversions and reactions and herein, the manuscript reviews some recent advancements and achievements in using nanomaterials as nanocatalysts. Many different methods are there to synthesize different nanomaterials and those preparative techniques can be used to synthesize different nanocatalysts, the present work reviews literature of such techniques and their recent applications with modification in previous synthetic methods. Such nanomaterial preparative methods when applied to nanocatalysis can be given a term called '*Nanocatalyst synthetic techniques with a twist*'. The aim to discuss such techniques is to make researchers understand the interdependence concept and using the pre-existing for new developments in nanocatalysis.

Keywords: Nanocatalysis, Nanomaterials, Quantum dots, Nanoskiving, Near field electrospinning

I.   Introduction

Now-a-days, scientists and engineers are making continuous efforts to develop new and different techniques to produce materials at the nanoscale so as to have benefits from their (nanomaterials) improved properties of higher strength, lighter weight, increased control of light spectrum, increased surface to volume ratio [1], high electro-conductivity, larger surface area and these properties can be put to use in uncountable usages like in biohydrogen production from cellulosic materials [2]; different carbon based nanomaterials, like grapheme, carbon nanotubes (CNTs), carbon quantum dots, carbon nitride dots, graphene quantum dots (GQDs) and graphitic carbon nitrides (g-C34) have been studied for their application as intrinsic peroxidase enzyme-like activity and as glucose bio-sensors [3]. Many organic polymer based, carbon based, transition metal/ metal oxide/ metal sulfide based nanomaterials have found to be effective in treating water for organic pollutants [4]. Nanomaterials have shown great effectiveness in studying the toxicity of arsenic and the principles, strategies, mechanism behind the nanomaterials involved in arsenic analysis has been efficiently reviewed by Xu *et al.* in their review [5].

So how we know that what is the importance of nanomaterials now and in recent future? Talk any new thing like any new technology and the nanomaterials are the spot attention seekers. This goes flawlessly true when studying a new scientific breakthrough in nanomedicine i.e. Nanotheranostics involving treatment for different cancer autoimmune, neurodegenerative and cardiovascular diseases [6]. Recently, lead bromide based tubular pervoskites has been studied as potential material with commercial application to be used in optoelectronic devices removing the pre-existing barriers of low external quantum efficiency (EQE), low photoresponsivity, smaller band gaps shown by CNTs, TiO_2, CdS, and ZnO [7]. MXene $(Ti3C2Tx)$ derived nanomaterials have their application in renewable energy conversion and storage like HER (hydrogen evolution reaction), in Li-ion batteries, in supercapacitors and in photocatalysis [8].

Nanocatalytic activity of many pre-synthesized/ in-situ iron oxide nanomaterials have been studied for a wide range of conversions including CO oxidation to CO_2, decomposition of hydrogen peroxide, ammonia decomposition, oxidation of water under visible light, alkylation reactions, oxidative esterfications and many organic compound synthesis like pyranopyrazoles, benzthioxazinone derivatives etc. [9]. Pd, Pt, Au, Ni, Ag, Cu and Cu Ni as single atom supported nanomaterials have been shown effective nanocatlytic activity[10]. Recently, Au22(L8)6

nanocluster protected by diphosphine moiety has been reported as an effective nanocatalyst in oxygen activation and CO oxidation reaction [11].

As we have seen how much importance does nanomaterials have, here in this review, the focus is on how nanomaterial, their synthesis and nanocatalysis are interdependent. The nanomaterials synthesized may be for different purposes can be explored for catalyzing reactions, thus can serve the role of nanocatalyst. On the other hand, nanocatalysts prepared are basically the nanomaterial and can be explored for different purposes. In past, six to seven years, nanocatalysis has achieved great work and near future still has its demand for the very usual reasons of 'nano' as has already been cited above. Everyone is in a race to construct new material/ catalyst/ techniques leaving behind the thought to make the usage of already existent. Now, taking this interdependence concept to preparative techniques, we can always use the techniques used for preparing nanomaterials of different applications for the production of nanocatalyst. Thus these techniques will be called as '*Nanocatalyst synthetic techniques with a twist*'. The techniques discussed in this review, has been reviewed on an individual level before but not combined with a thought of blending the two: material and catalysis concept. In this context to nanocatalysis, there are many nanomaterials that can be used effectively as nanocatalysts depending upon different size, shapes and dimensions but the present work reviews recent work and advancement of some of the types based on the nature of material and irrespective of their size, shape and dimensions.

II.   Some potential nanomaterials for nanocatalysis

Some of the different types of nanomaterials that have the potential to be used for nanocatalysis are:
1.1   Carbon nanotubes;
1.2   Graphitic carbon;
1.3   Heteroatom doped carbon;
1.4   Metal Nanoparticles;
1.5   Silica nanomaterials;
1.6   Titania based nanomaterials; and
1.7   Zirconia based nanomaterials
1.8   Quantum Dots
1.9   Aerogels

2.1   *Carbon nanotubes (CNTs):* CNTs have gathered a lot of attention because of their unique mechanical and physical properties. Inspite of being used as a nanocatalyst in organic synthesis, CNTs have also been appplied in many fields such as these are used in electric nanoconductors, in fuel cells, in electric double layer capacitors and in lithium ion secondary batteries. Luo *et al*. reported a synergistic effect of platinum/ yttrium coated and pyridine-functionalized multi-walled carbon nanotubes toward the reduction of oxygen reduction in acid medium [12]. Riberio *et al*. emphasized upon the utility of carbon nanotubes as additives in the oxidation of 1-phenylethanol (Scheme 1) [13]. Gunbatar *et al*. reported multiwalled CNTs based Rh nanoparticles for the effective hydrolytic dehydrogenation of dimethylamine borane (DMAB). The nanocatalyst has shown a catalytic TOF value of 3010.47 h^{-1} along with its complete kinetic study (Scheme 2) [14]. Rather *et al*. reported multi-walled CNTs supporting La/Ce mixed oxide nanoparticles have been efficiently used and recyclability have also been studied in the synthesis of chromeno pyran derivatives under eco-friendly parameters *viz*. terms of atom economy, E-factor, overall efficiency etc. (Scheme 3) [15].

Scheme 1.

$$(CH_3)_2NHBH_3 \quad + \quad 2\,H_2O \quad \xrightarrow[RT]{RhNps@MWCNT} \quad [(CH_3)_2\,NH_2]\,[BO_2] \quad + \quad 3\,H_2$$
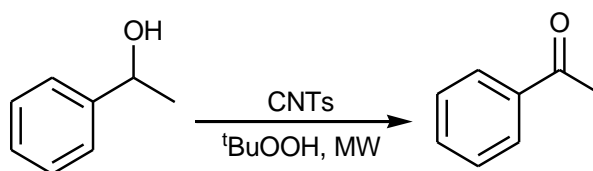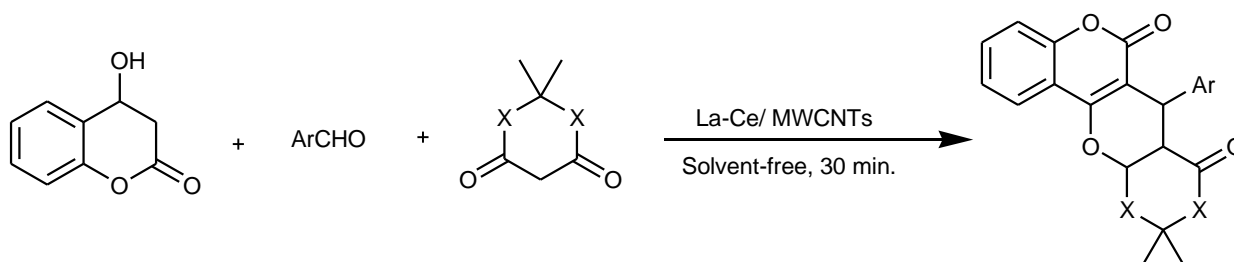
Scheme 2.

Scheme 3.

2.2 *Graphitic carbon*: Sohn *et al.* observed the synthesis of TiO_2 graphitized carbon composites and its application as anodes in Li-ion batteries [16]. Chen *et al.* too reported Ni-diffused graphitic carbon as anodes in Li-ion batteries [17]. Wang *et al.* reported the dehydrogenation of ethyl benzene using nickel based hybrids of graphitic carbon [18]. Verma *et al.* reported the magnetic graphitic carbon as an efficient catalyst in the C-H activation of amines (Scheme 4) [19]. Chabbra *et al.* have developed sulfonated graphitic carbon nitride and used it as an efficient recyclable and sustainable catalyst for the transformation of various biomass derived sachharides like starch, sucrose, fructose and cellobiose to a highly value added product i.e. 5-hydroxymethylfurfural, that serves as a chemical for biodiesel and other fuels [20]. Yu *et al.* have exfoliated graphitic carbon nitride (g-C_3N_4) and used it as a supporting material to support $FeCl_3$ and found that exfoliation of graphitic nitride has improved the surface area and pore volume for stable anchoring of $FeCl_3$. The catalyst prepared by them has shown high activity and selectivity in hydroxylation of benzene with a maximum phenol

yield of 22% at 60 $^{\circ}$C under H_2O_2 (Scheme 5) [21]. Ergen *et al.* have defined the usage of recyclable mesoporous graphitic carbon nitride (mpg-C_3N_4) to support AgPd alloy nanoparticles to act as an effective catalysts for one-pot synthesis of secondary amines using a tandem reductive amination approach to variable aldehydes with nitroarenes in water giving an yield of upto 99% (Scheme 6) [22]. Shcherban *et al.* used melamine derived graphitic carbon nitride with TEOS as a hard template to be an effective catalyst in Knoevenagel condensation of benzaldehyde and ethylcyanoacetate yielding ethyl-α-cyanocinnamate (upto 51%) which was the best catalyst for conversion amongst other C_3N_4-Ar, C_3N_4-Air and N-doped C_3N_4 comparative counterparts (Scheme 7) [23].

Beyond graphene, the other elements in the same group *viz.* silicene, germanene and stanene [24] materials have also been prepared and studied through different characterization techniques. These materials leave scope for future experimentation in nanocatalysis.
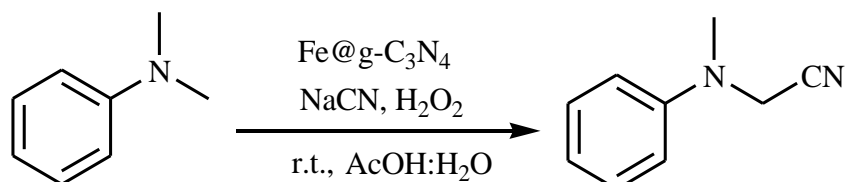
Scheme 4.
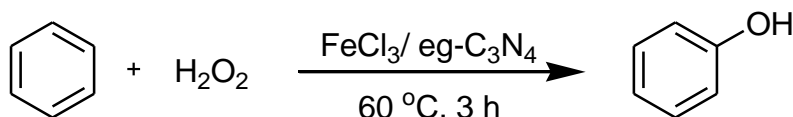
Scheme 5.
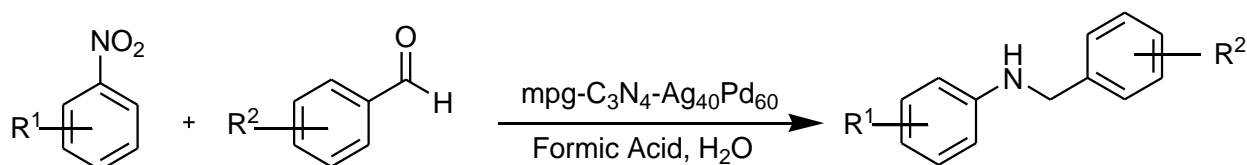
Scheme 6.
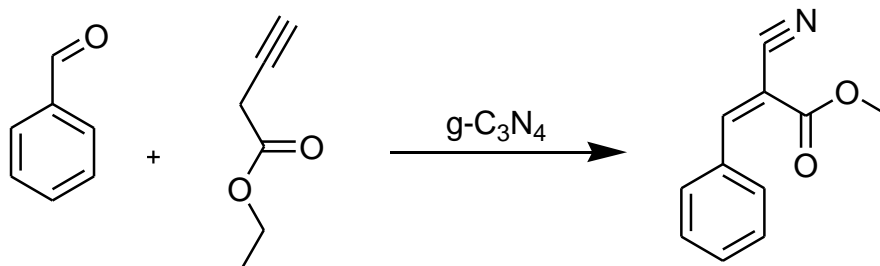
Scheme 7.

2.3 *Heteroatom doped carbon*: Doping of heteroatoms in carbon materials increases the scope of application by altering the different properties of the undoped material. This leads to their use in supercapacitors [25,26], fuel cells [27,28], batteries [29,30] and water splitting [31], oxygen reduction reaction (ORR) [32], hydrogen evolution reaction (HER) [33], field emission and so on [34]. Molla *et al*. studied the direct transformation of aryl halides to benzyl alcohols using palladium nanoparticle encapsulated nitrogen doped mesoporous carbon material (Pd@N-GMC) as a catalyst (Scheme 8) [35].
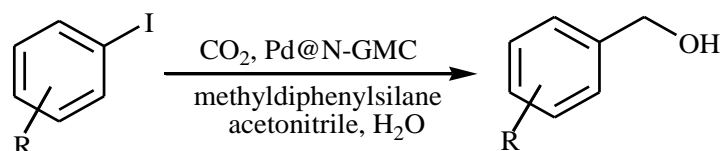
Scheme 8.

Li *et al*. have discussed the pyridinic N as the most active species responsible for oxidative desulfurization in *N*-doped nanoflakes prepared by them. They have claimed *N*-doping and certain structural defects were responsible for H_2S selective oxidation with a high catalytic performance of around >740 $gsulfurkgcat.^{-1}h^{-1}$ [36]. Phosphorous doped CNTs have been explored by Yuan *et al*. for an efficient metal free synthesis of ammonia using electrochemical nitrogen reduction reaction (NRR) giving a noticeable yield of 24.4 $\mu gh^{-1}mg^{-1}$ cat. and partial current density of 0.61 $mAcm^{-2}$ [37].

Nitrogen and Boron doped carbon ($Co_2B/Co/N$-B-C/B_4C hybrid) has been successfully studied as an efficient catalyst for oxygen reduction reactions, hydrogen evolution reactions, oxygen evolution reactions as reported by Liu *et al* [38] and as a catalyst (Fe/BCNNS) for electrochemical CO_2 reduction by Ghosh *et al* [39] using a proton exchange CO_2 membrane cell. Brandi *et al*. have presented a sustainable pellet shaped Ni nps supported on nitrogen doped carbon as a nanocatalyst in the aqueous phase hrdogenation of lignocellulosic biomass-derived compounds using a continuous flow system [40].

2.4 *Metal nanoparticles*: Both bare metal nanoparticles as well as supported metal nanoparticles have been studied as nanocatalysts in catalyzing effectively various synthetic conversions. Rhodium (0) nanoparticles supported on covalent triazine-based framework (Rh@CTF^{-1}) obtained from 1,-dicyanobenzene has been put to use an efficient catalyst for hydrogenation of benzene to corresponding cyclohexane with conversion of upto 99% under mild (10 bar, H2, 70 ºC) solvent-free conditions with a recyclability of the nanocatalyst for consecutive ten runs by Siebels *et al*. Moreover, Rh@CTF^{-1} has proven as an electrocatalyst for hydrogen evolution reaction (operating potential = -58 mV) (Scheme 9) [41]. Wastes produced from petroleum production is a matter of concern and Saha *et al*. made an attempt towards curbing the problem by synthesizing and studying the effect of binaphthyl stabilized platinum nanoparticles (Pt-

BNP) in selective and controlled oxidation of alkylarenes using TBHP as a greener oxidant in water. The nanocatalyst have shown high turnover numbers (TON) of 738-1448 with reusability upto five runs (Scheme 10) [42]. Mohire *et al.* have synthesized hydrocinnamaldehyde, a perfumery compound from selective C=C over C=O hydrogenation of cinnamaldehyde using a reusable reduced graphene oxide supported Cu-Ni nanocatalyst (Ni:Cu ratio = 1:1) in methanol at 150 ºC under 20 atm. pressure (Scheme 11) [43]. Cobalt

nanoparticles supported on *N*-modified carbon(Co/Melamine- 2@C-700) has been studied by Chen *et al*. for transfer hydrogenation of variable quinolenes and different *N*-heteroarenes with a product yield of upto 98% in toluene at 130 ºC using formic acid as a hydrogen source(Scheme 12) [44]. Baharfar *et al.* reported the synthesis of benzothiazepine and spiro benzothiazine using lipase immobilized on Fe_3O_4 nanoparticles as catalyst (Scheme 13) [45].

Scheme 9.

Scheme 10.
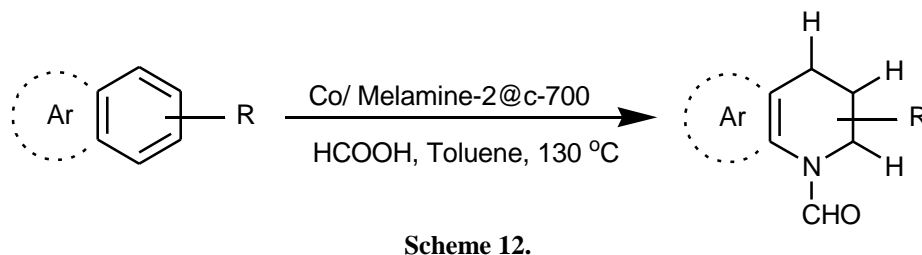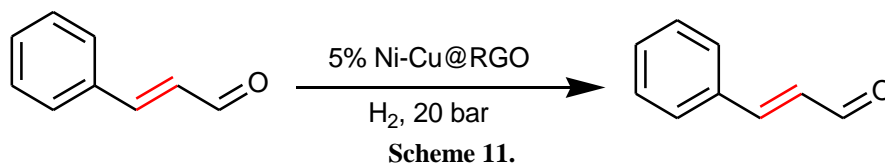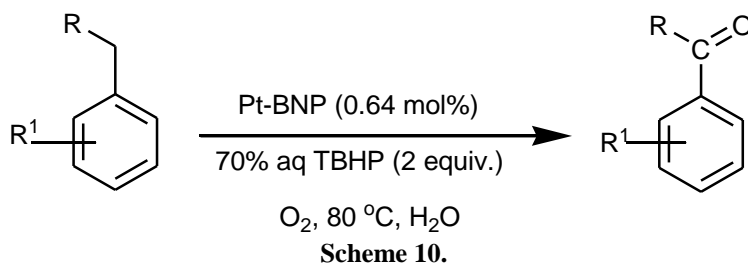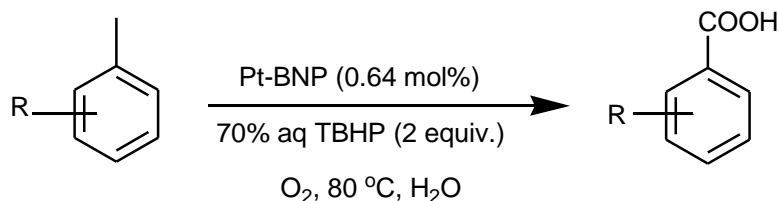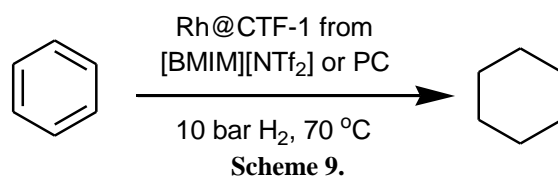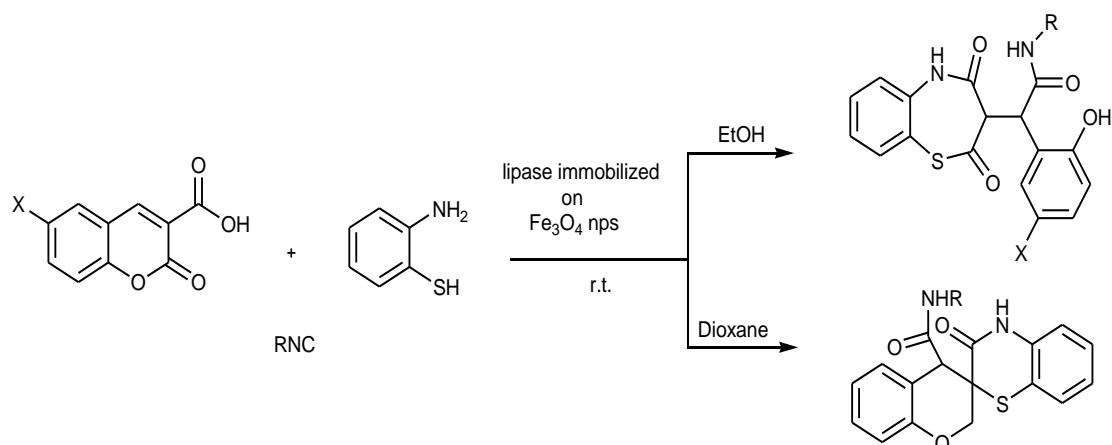
Scheme 11.

Scheme 12.

Scheme 13.

2.5 *Silica based nanomaterial*: Liu *et al.* have synthesized potassium modified stannous containing dendritic mesoporous silica nanoparticles (DMSNs) to study the dehydrogenation of propane to propylene wherein the researchers have claimed the dispersed SnOx to be the active site of dehydrogenation rather than polymeric SnOx and crystalline SnO2 species. The reaction process involved a cyclic mechanistic approach wherein the adsorption of propane took place on the surface of Sn-O-Si bonds and the active bridging oxygen sites abstracted the hydrogen from the methylene group leading to the formation of Sn-isopropyl intermediate along with the surface silanol groups. The intermediate species then undergoes a *β*-hydrogen cleavage to give the corresponding propene as a a product along with the generation of H_2 molecules from surface silanol groups, finally leading to the recovery of Sn-O-Si bonds (Scheme 14) [46]. Veisi *et al*. have used a green approach to synthesize a recyclable green tea extract encapsulated silica gel decorated with Pd nanoparticles as a nanocatalyst for the Buchwald-Hartwig C-N coupling reactions and the nanocatalyst has shown excellent yield upto 96% when different substituted aryl halides were reacted with different secondary amines over the nanocatalyst (Scheme 15) [47]. Alkyl esters are useful intermediates for the production of biofuels, polymers flavours, perfumes and esterfication has been one of the most important reaction for their synthesis. Considering its importance Abaoelhassan *et al.* have studied the esterfication of linoleic acid using reusable sulfonic acid functionalized silica nanoparticles (SiO_2NPs) and found it to be an excellent catalyst with a conversion rate of 100 %, TOF values from 53-498 h^{-1} with rate constants in a range of 1.80-5.55 h^{-1} [48].
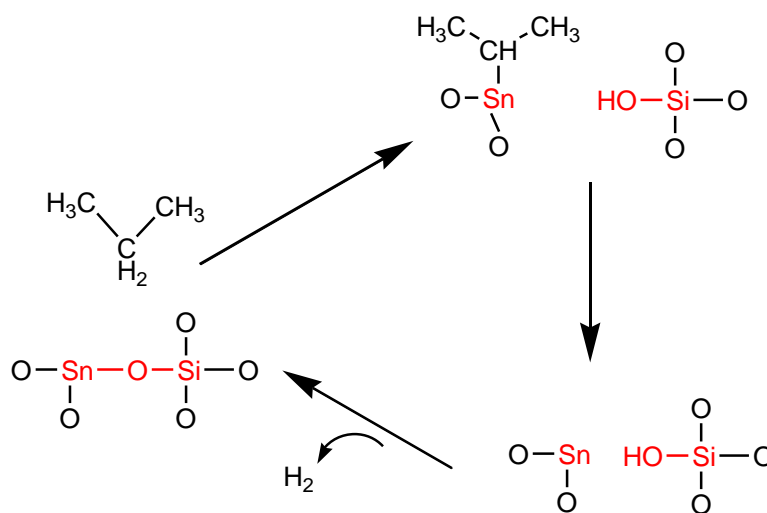
Scheme 14.
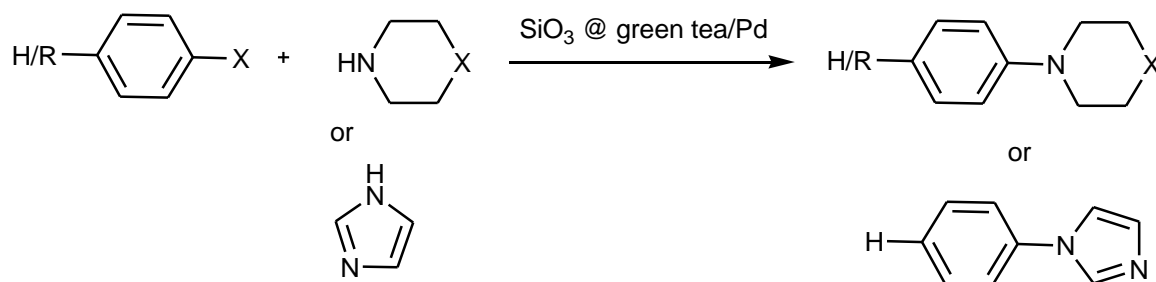
Scheme 15.

3.7 *Titania based nanomaterials*: Recently Kumar *et al.* have reported the application of hollow Au@TiO$_2$ nanofibres as an effective nanocatalyst in the reduction of 4-Nitrophenol to the corresponding 4-aminophenol as well as in the degradation of organic dye viz. Congo dye in the presence of sodium borohydride. They have found the catalyst to be quite reusable in both the reactions without any significant loss in activity on reusage [49]. Ledesma *et al*. have synthesized iridum supported on Titania modified CMK-3 nanomaterial (Ir-Ti-CMK-3) and studied it as an efficient catalyst for the hydrodenitrogenation (HDN) of indole to give indoline (HIN), o-ethylaniline (OEA), ethylbenzene (EB) and ethylcyclohexane (ECH) which accounted for above 98% of the total products. They have found that hydrodenitrogenation of indole was much

efficiently catalyzed by Ir-Ti-CMK-3 and in lesser time than when Ir-CMK-3 not modified with titania was used as a catalyst [50]. Kour *et al*. have reported the one-pot multicomponent synthesis of indeno[1,2-*b*]indole-9,10-diones (upto 94% yield) and 1*H*-pyrazolo[1,2-*b*]phthalazine-5,10-diones (upto 95% yield) in water using a long chain ionic liquid coated sulfonated carbon-tiatania composite (C@TiO$_2$-SO$_3$H-ILs) as an efficient and reusable catalyst. The reusability was observed for consecutive five runs (Scheme 16) [51]. Usage of titania nanomaterials has also been observed in the synthesis of dihydrocarvones Demidova *et al.* using a titania supported gold catalyst *via*. a selective one-pot hydrogenation of carvone oxime (Scheme 17) [52].
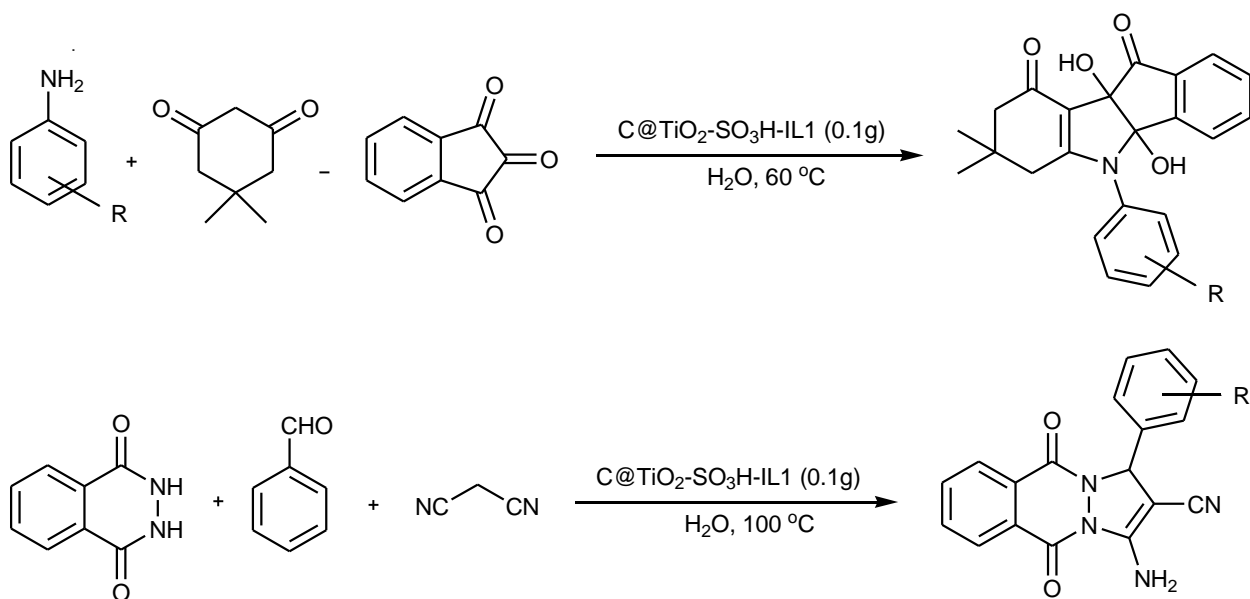
Scheme 16.
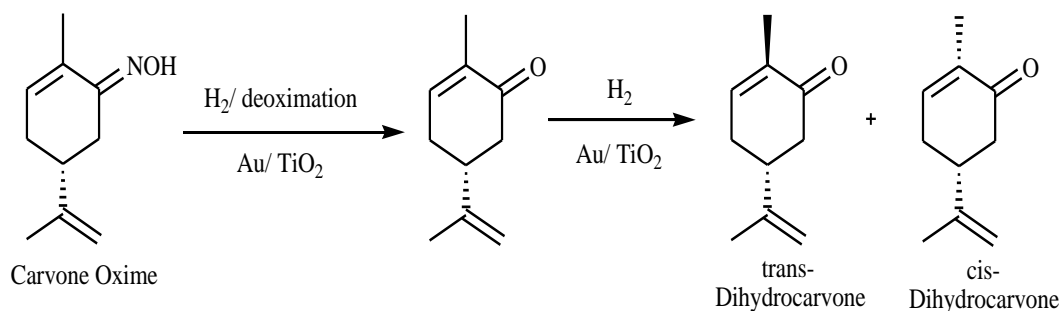
Scheme 17.

3.8 *Quantum Dots*: These nanocrystals having unique electronic properties can produce distinctive colors due to fluorescence have also been studied to serve as nanocatalyst. Yang *et al.* prepared Ag modified CQDs (carbon quantum dots) and found its excellent nanocatalytic ability in cyclohexane oxidation under visible light due to synergistic interaction between Ag nps and CQDs. The reusability for ten consecutive run shows its effectiveness as a nanocatalyst (Scheme 18) [53]. Mohammadi et al. observed the nanocatalytic activity of tungstate ions supported on 1-aminopropyl-3-methyl-imidazolium chloride ([APMim][Cl]) modified CQDs (CQDs@IL/Cl−) in the oxidation of various primary, secondary and other alcohol substrates to corresponding aldehydes and ketones in higher yields with 100% selectivity (Scheme 19) [54].

KA oil
Selectivity 95.2%
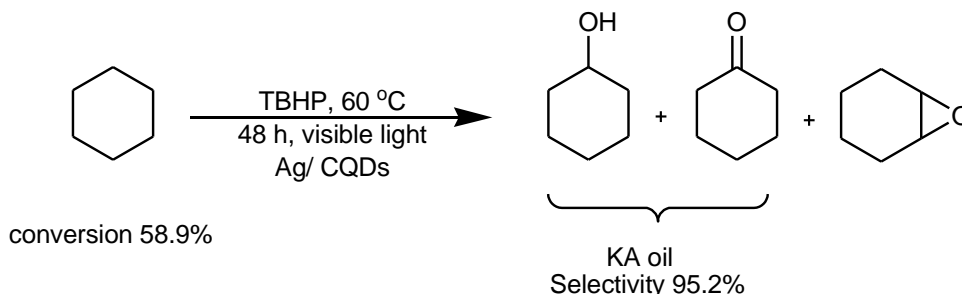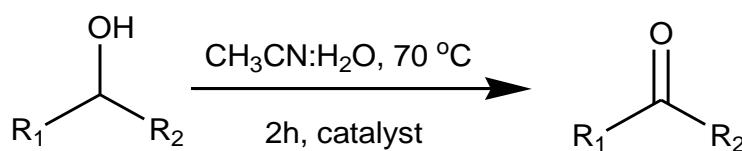
Scheme 18.

Scheme 19.

Li *et al.* have synthesized N-doped carbon dots (CDN) with strong fluorescent nature using a microwave irradiation method and studied its nanocatalytic role in the fluorescence reaction of 3,3,5,5-tetramethylbenzidine hydroxide ((TMB)–H_2O_2) producing TMBOX as an oxidizing product of the reaction (Scheme 20) [55]. Mahmoudabadi *et al.* have studied the effective nature of unsupported MoS_2 quantum dots (M-QDs, 0 ppm sulfur) prepared through exfoliation and dispersion of MoS_2 as a nanaocatalyst in hydrodesulfurization of naptha [56].
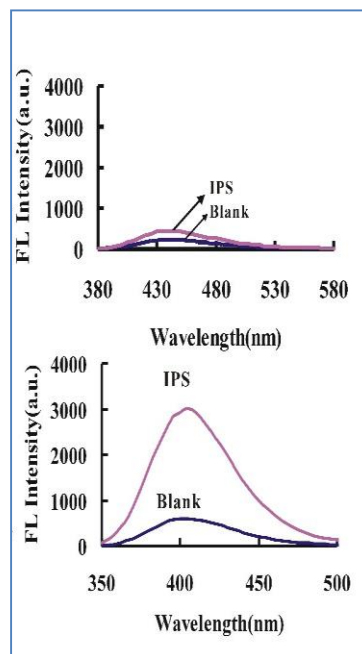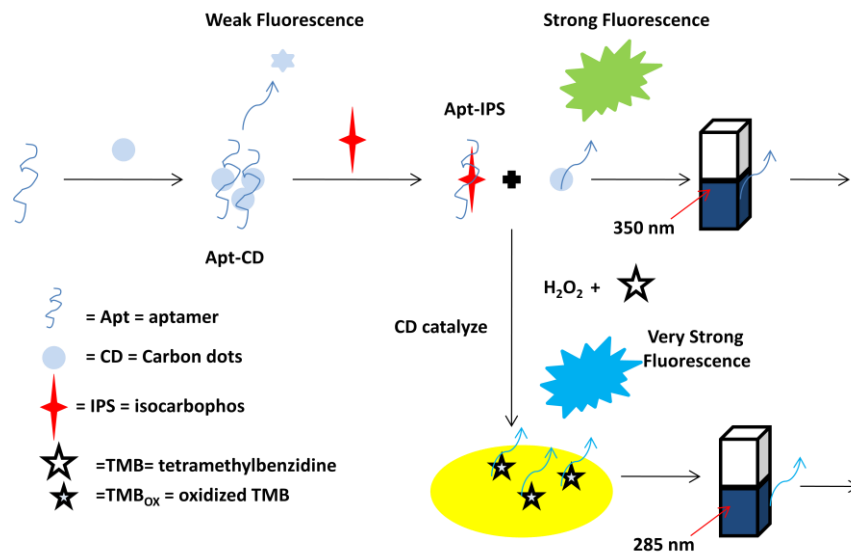
Scheme 20.

3.9 *Aerogels* and *Xerogels*: These extremely low density solid materials synthesized by removing the liquid component from a conventional gel have also been studied for their nanocatalytic activity. Tesfaye *et al*. have shown the Ni-Co bimetallic nps supported on CNT aerogels working as anode material as an efficient nano electrocatalyst synthesized by a polyol reduction and sol-gel methodology for urea oxidation reaction (UOR) [57]. Recently Yang *et al*. have reported high catalytic activity of Pd-Ru bimetallic nanocatalyst synthesized by Pd induced aerogel for striking release of H_2 from ammonia borane hydrolysis

[58]. Rhodamine 6G is used as a colour enhancement for pigment inks in textile industry and is considered to be an environmental pollutant. Minati *et al*. have discovered the usage of Pd functionalized graphene xerogel (GX-Pd) nanocomposite in the reduction of Rhodamine 6G and the reaction was studied using UV analysis showing discolouration of the Rhodamine 6G when GX-Pd was added to it in comparison to sodium borohydride which never responded to the reduction reaction even after being as a strong reducing agent (Scheme 21) [59]. Silica xerogels have also been explored as an electrocatalytic

sensor when doped with Ba^{2+} and Eu^{3+} giving a redox potential of 0.06 V due to Eu redox sites in silicates and the success of the design was confirmed by the increasing anodic peak current due to isoniazid oxidation [60]. TEOS (tetraethylorthosilicate) modified xerogels

decorated with silver nanoparticles have also been explored by us as a successful recyclable nanocatalyst in the synthesis of benzopyranopyrimidines and in the synthesis of *gem*-bisamides giving an yield of upto 93% (Scheme 22) [61].
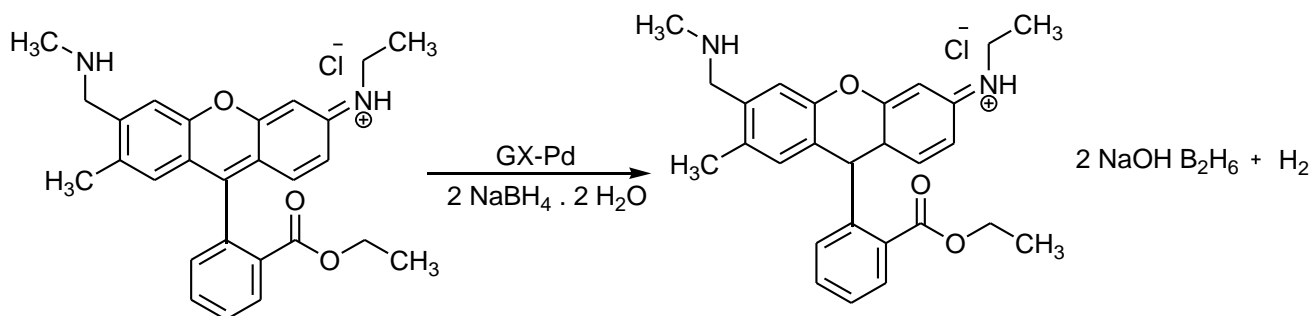
Scheme 21.
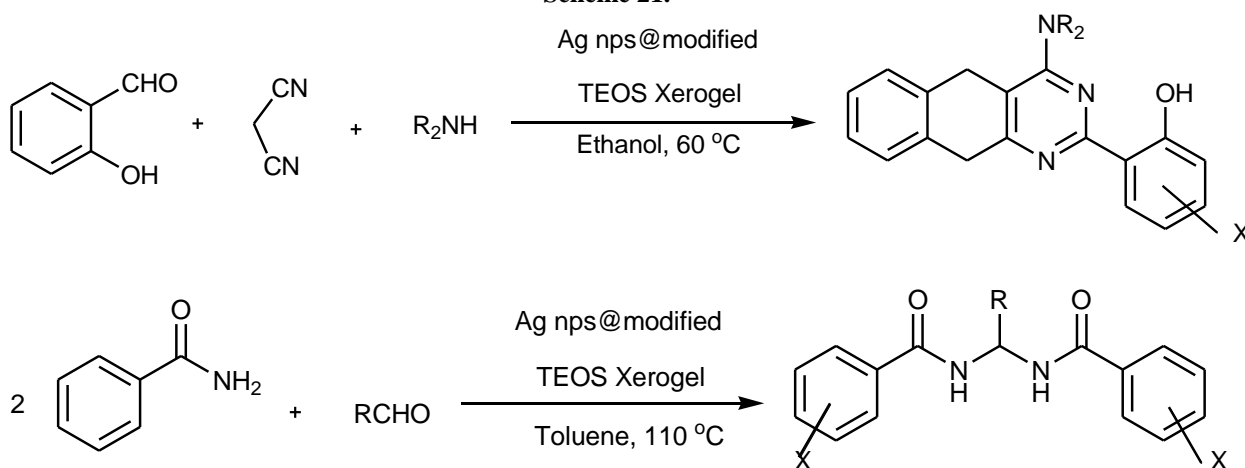
Scheme 22.

III.   Nanocatalyst synthetic techniques with a twist and recent devlopments

Molten Salt Method: Originally used for the synthesis of ceramics, this method made a way to be used in synthesizing nanomaterials of different importance. The method generally involves the heating of a low melting salt along with reactants to a temperature above the melting point of salt wherein the molten thus formed serves as a solvent. This molten mass after cooling gives a powdered product which is washed with solvent (usually water) to remove the unreacted salt and the characteristics of the material obtained can desirably be controlled by controlling the heating temperature and the time of heating. Very recently, Mao and co-workers has utilized this methodology and named it as *Dopant Replacement Driven-Molten Salt Method*

(DRD-MSM). Herein this methodology, they have used sodium nitrate as the molten salt and a mixture of ammonium molybedate tetrahydrate, ammonium tungstate hydrate were used as reactants. The heating was done with the aid of a furnace at a constant temperature set to 380 ºC with a reaction time of few seconds. Storage of the nanomaterial has been studied as a dispersion in water. Confirmation of the prepared nanomaterial has been done using techniques like Transmission electron microscopy (TEM) and high resolution TEM (HRTEM) studies which showed the formation of individual nanowires of dimensions 3.5-4.5 nm dia., ≈300-500 nm length and a lattice spacing of 0.385 nm. SAED (selected-area electron diffraction) pattern showed diffraction patterns corresponding to 001 and 220 planes, thus confirming the crystalline

nature of the nanowires. Powder XRD studies confirm peaks at 23.6º and 28.2º corresponding to 001 and 220 plane. X-ray photoelectron spectroscopy (XPS) analysis suggest the presence of Mo along with W, O and C. High resolution XPS spectra of 4 f core levels of W showed two well separated peaks at 35.42 eV and at 37.51 eV with no shoulder peaks present in the region. Mo 3d core levels showed two spin-orbit doublets due to co-existence of Mo^{5+} and Mo^{6+} . O1s XPS spectra showed three different peaks at 530.28 eV, 531.97 eV and 533.35 eV confirming oxygen in three different environment comprising of O in W-O-W lattice, as a surface bonded hydroxyl group and as present in adsorbed water molecules. O K-edge X-ray absorption near edge structure (XAENS) showed greater M-O bond covalency by observing an intense peak at ≈533eV due to electron transition from 1s-orbital of oxygen to d-orbitals of W or Mo. The advantage of this method lies in the fact that the nanowires can be prepared in less than 1 min. of reaction time [62]. He *et al*. have reported KSCN molten salt technique to produce hetero-structures of MoS_2 and CoS_2 (MoS2@CoS2) under low temperature conditions for a high performance hydrogen evolution reaction (HER). The benefit as well as the difference from traditional method lies in non-usage of additional source of sulfur. The method claims its advantage for a practical use by offering features like low cost of KSCN, high stability, providing a low overpotential of 96 mV at 10 mA cm^{-2}, a low-temperature synthesis avoiding destruction of energy sites by induced high temperature conditions and a suitable ΔGH* value for a significant catalytic performance in HER [63]. Wang and co-workers have used molten salt technique to prepare phosphorescent carbon dot based nanocomposite which show a tunable color feature at room temperature and is ideal for its application high level information anticounterfeiting using a dual security protection strategy [64]. The molten salt strategy has been well exploited for the synthesis of very usable silicon nanoparticles by making good choice of eutectic salt as a solvent, ideal alkoxide as a precursor and using an ideal rare earth metal as a stabilizing agent [65].

Near Field Electrospinning: Originally the method was designed for printing technology using electric field. In this method, a solid tungsten probe (tip diameter of approx. 25 mm) was used as a spinneret, a stable jet used for the deposition of controllable electrospun nanofibres, an electrode and a collector set at a very small distance of 500 mm to 3 mm (approx.) are used. In the NFES experiment, the electrode-to-collector distance was shortened to the range of 500 mm to 3 mm, and the stable jet could be utilized to achieve the controllable deposition of electrospun nanofibers. A solid tungsten probe with a tip diameter of 25 mm was used as the spinneret to replace the hollow nozzle in traditional electrospinning. The initial diameter of the charged jet that ejected from the spinneret was smaller than the diameter of the tip, which promoted the evaporation of solvent and helped to gain a solid uniform nanofiber with diameter ranging from 50 to 300 nm. The spinneret helps in achieving increased strength of the electrical field and enhace the stability of charged jet. A shortened distance between the electrode and the collector ensures the deposition of nanofibre precisely onto the collector. A straight jet serves an electrospinning of a predesigned pattern by keeping a check on the motion trajectory of the collector. The whole process is operated under microscope observation which helps to attain an improved electrospinning pattern and this supports its application to nano fabrication [66]. NFES based 3D nanoprinting process has been used to produce self-aligned, 3D stacked template-free nanostructures (curved nano walls, nanobridges and nano "jungle gyms"). The modified method shows a potential to achieve precisely controlled layer by layer deposition of nanofiber by a simple addition of a salt to PEO (polyethylene oxide) solution and the results gave printing of 92 ± 3 to 239 ± 30 nm thickened nanowalls with aspect ratios (h/w) in a range of 48-72 pertaining to different salt concentration in PEO solution. Such nanostructures have been further studied for application in nanoelectronics as templates for the patterning of nanoelectrodes using controlled electrical resistances [67]. Smart electronic products are on high demands and *Y*-Fe_2O_3 nanoparticles embedded polymeric fibers have recently been explored as a new family of high-performance and flexible electromagnetic shielding materials. Herein, the modification to the pre-existing electrospinning method is the usage of magnetic field which helped in lowering the voltage usage in usual NFES method. A fixed 1% Y-Fe_2O_3 nanoparticles mass ratio under 93 mT magnetic field suggested the formation of ideal material. TEM micrographs (Figure 1) have shown the uniform size of Y-Fe_2O_3 nanoparticles with no agglomeration inside and outside along with 700 nm dia. nanofibres; FTIR spectra gave characteristic peaks of PVP in composite material showing no change in polymeric structure due to the presence of Y-Fe_2O_3 nanoparticles; XRD gave usual peaks at 30.7º, 36.1º, 44.7º, 54.8º, 57.6º and 64.8º

corresponding 220, 311, 400, 422, 511 and 440 crystal planes of γ-Fe$_2$O$_3$ nanoparticles; XPS confirmed the purity of γ-Fe$_2$O$_3$ in the sample and molding the sample with tweezers under the

influence of magnetic field without any breakage confirmed the elasticity of the material produced [68].
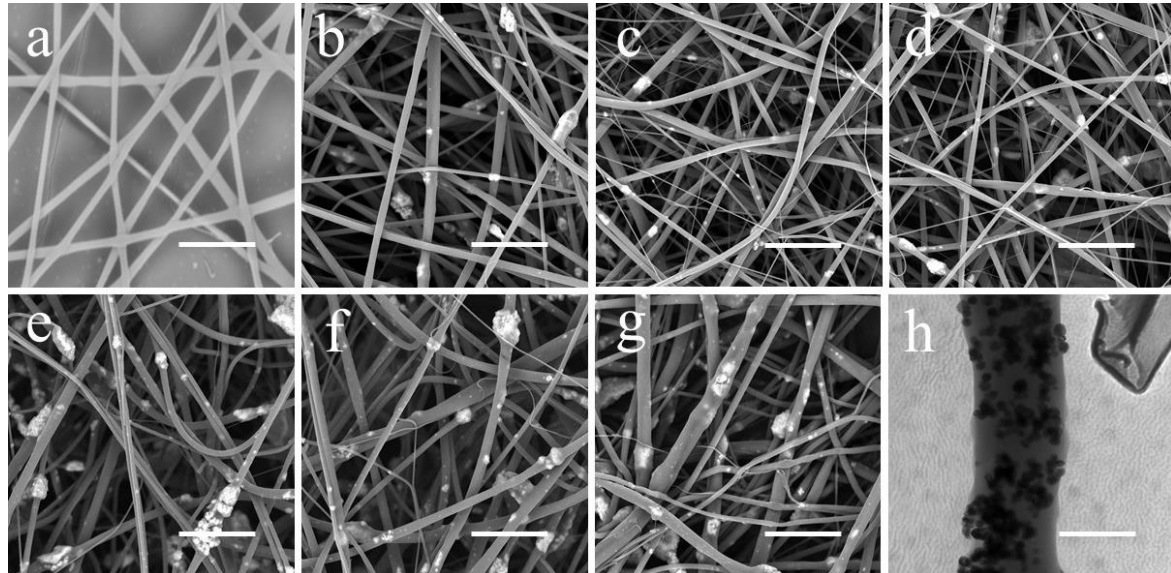
Figure 1. Scanning Electron Microscopy (SEM, scale: 5µm) images of nanofibres fabricated using Near-Field Electrospinning (NFES) Technique without using a magnetic field: (a) PVP and (b) PVP/ ν-Fe$_2$O$_3$ nanofibers; naofibres fabricated using Magnetic Electrospinning (MES) Technique: (c–g) PVP/ ν-Fe$_2$O$_3$ nanofibers ; (c–e) PVP/ ν- Fe$_2$O$_3$ nanofibers with 1 wt % mass ratio of ν-Fe$_2$O$_3$ at different magnetic field strengths i.e. (c) 30 mT, (d) 93 mT and (e) 154 mT. PVP/ ν-Fe$_2$O$_3$ nanofibers synthesized at 93 mT magnetic field strength with different mass ratios of ν-Fe$_2$O$_3$: (f) 2 wt % and (g) 3 wt %. (h) Transmission Electron Microscopy (TEM, scale: 600 nm) image of PVP/ ν-Fe$_2$O$_3$ nanofibers fabricated using Magnetic Electrospinning (MES) with a mass ratio of 1 wt % and a magnetic field strength of 93 mT. Pictures taken from *Polymers*, 2020, *12*, 695. Published by: MDPI.

Nanoskiving: This method involves thin films deposition on polymeric substrates like poly (dimethylsiloxane) that are topographically patterned with the help of physical vapour techniques along with sectioning using an ultramicrotone. The steps involved are: i) Casting an epoxy prepolymer (for eg., Araldite 502) on a topographically patterened polymeric substrate like PDMS [poly (dimethylsiloxane) stamp]; ii) Deposition of metallic thin film on topographically patterned epoxy using different deposition techniques leading to the formation of layers having thickness in nanometers. The above arrangement is then further embedded in additional epoxy layer to give an epoxy block having metallic thin film embedded in it; ii) From the above block, slabs of around 30 nm thickness are sliced using ultramicrotome technique and the sectioned slabs float on the water surface in the collecting reservoir of the ultramicrotome; iv) The epoxy section from each slab is then separated from the embedded

metallic thin film by using oxygen plasma leading to nanosized metallic films and finally the dimensions *viz.* **x** , **y** (thickness of deposited film) and **z** (thickness of the epoxy slab obtained by sectioning) are topographically determined. (Figure 2) explains the procedure [69]. Fang and co-workers very recently have reported the usage of nanoskiving to produce Au nanowires. Herein, epoxy blocks containing Au nanowires have been used and sliced into 30-200 nm thick sheets and transferred to pre-etched silicon groove which after fixing by platinum using focused ion beam (FIB) results into 88-200 nm width, 43-295 nm thick and 500 µm length Au nanowires. AFM and TEM studies have been used to study the topography. Using AFM studies, the average Youngs' modulus obtained for perpendicularly cut Au nanowire and parallelly cut nanowire are 77.2 ±9.5 GPa and 75.1 ±11.9 Gpa which showed a good agreement with the bulk gold's Young modulus i.e 78 GPa inferring no effect of size, thickness and direction

of cutting on the Young's modulus. TEM studies showed the effect of cutting direction on dislocations and ultrafine twins leading to an increased yield strength when direction of cutting is parallel as compared to when cutting done in perpendicular manner [70]. Nanoskiving has been used to fabricate 3D nanoantenna having zig-zag nanogaps at a defined angle for plasmonic nanofocusing in plasmonic devices [71]; to produce Au nanowire size controlled with variable shape electrodes for electroanalysis of oxidation of catecholamine [72] and to perform hydrodynamic voltametry. Single gold nanowire synthesized from nanoskiving technique when combined with polyimide tape have been studied for its sensor application by monitoring pulse pressure wave originated from the radial artery [73].
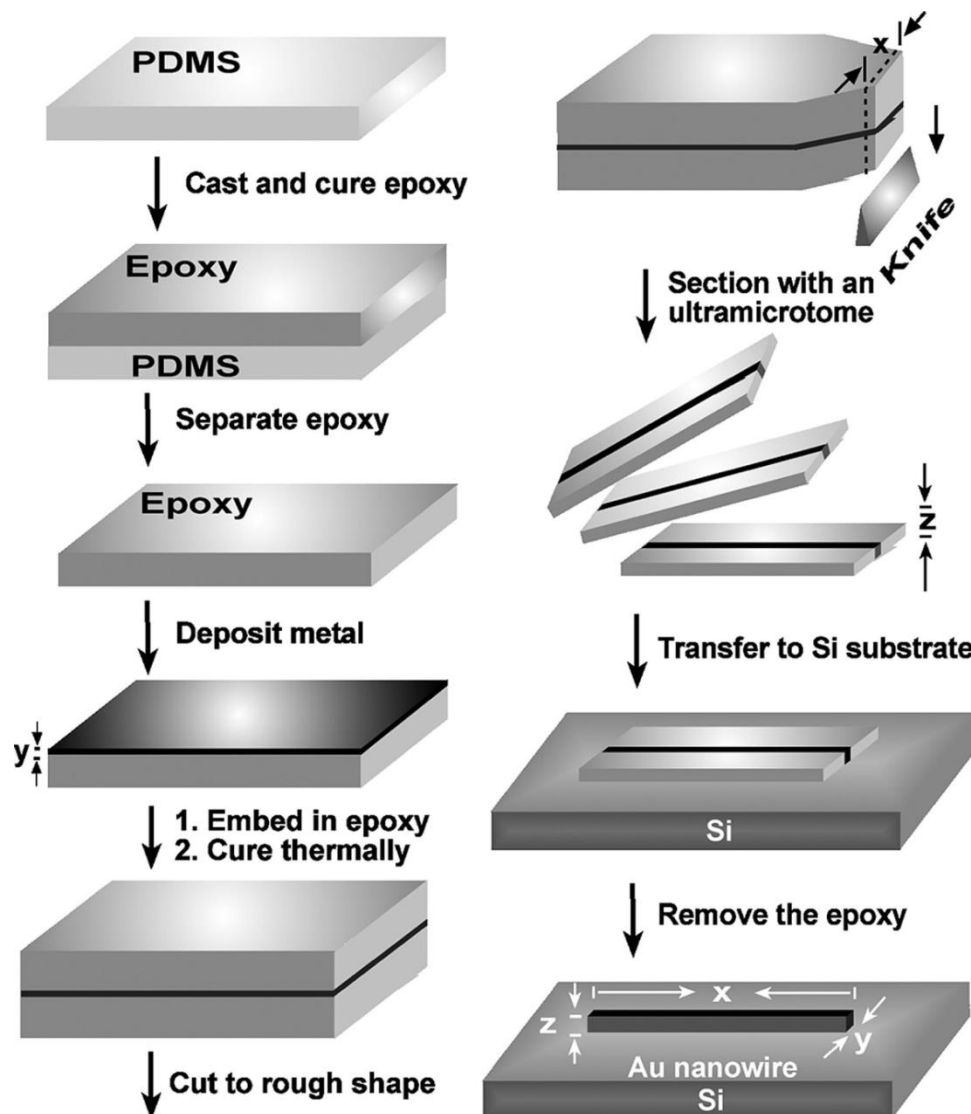
Figure 2. Fabrication of Au nanowires by nanoskiving. Picture taken from Accounts of Chemical Research, 2008, Vol.41, 1566-1577; Published by American Chemical Society.

Melt-Emulsion-Quench Approach: First reported by Tesfaii and co-workers for the synthesis of ionic liquid nanoparticles using solid 1-butyl-2,3-dimethylimidazolium hexafluorophosphate ([bm2Im][PF6], m.pt = 42 °C) as the key substrate. The methodology involved two pathways: *First* *Pathway:* Herein, the solid IL is melted and subsequently dispersed as o/w into water maintained at a temperature above the m.pt of IL. This emulsion is then subjected to subsequent cooling to produce discrete nanoparticles of the solid IL. *Second Pathway:* This pathway has a

difference of using nonionic surfactant Brij 35 as an emulsifier for the formation of IL nanoparticles. (Figure 3) [74]. Transparent, green colored chromium doped strontium alumino borate [(30-x) BaO-xAl$_2$O$_3$-69.5B$_2$O$_3$-0.5CuO)] glasses with a thickness of 0.5-1 mm have been prepared by using melt quench technique in which different melts with variable molar ratio of the constituents were prepared in electric furnace at 1100 °C; with further quenching of melts over a preheated (150 °C) steel plate with final annealing at 300 °C. The samples have been studied using techniques like XRD which showed absence of sharp Braggs' peak inferring amorphous nature of the glasses; densities were calculated using Archimedes principle which showed a decrease in the density with increase in molar volume as the alumina molar ratio increases; a single broad absorption band centered at 785 nm due to $^2B_{1g}$ $^2B_{2g}$ Cu^{2+} in optical absorption spectra has been observed and EPR spectrum gave three weak parallel components in the lower field region along with fourth parallel component overlapped with perpendicular component which signifies the presence of Cu^{2+} centers to occupy octahedral symmetric sites [75].

Shukla *et al*. have studied the dielectric properties of chalcogenide glassy alloys of Se90Cd10-xlnx (x = 2, 4, 6, 8) prepared by melt quench technique using impedance spectroscopy (ν = 42 Hz – 5 Hz, RT) which showed that for all compositions at RT, the real and the imaginary part of dielectric constant decrease with increase which is attributed to contribution of multi-components of polarizability, electronic and ionic deformations orientational and interfascial polarization. Also a decrease in tan with frequency which infers the mobility of charge carriers upto some distance in the glassy alloys in the presence of applied electric field. AC conductivity dependency of the melt quenched glassy alloys with frequency have also been studied and an increasing trend of AC conductivity with increasing frequency is attributed to an enhanced conduction mechanism [76].
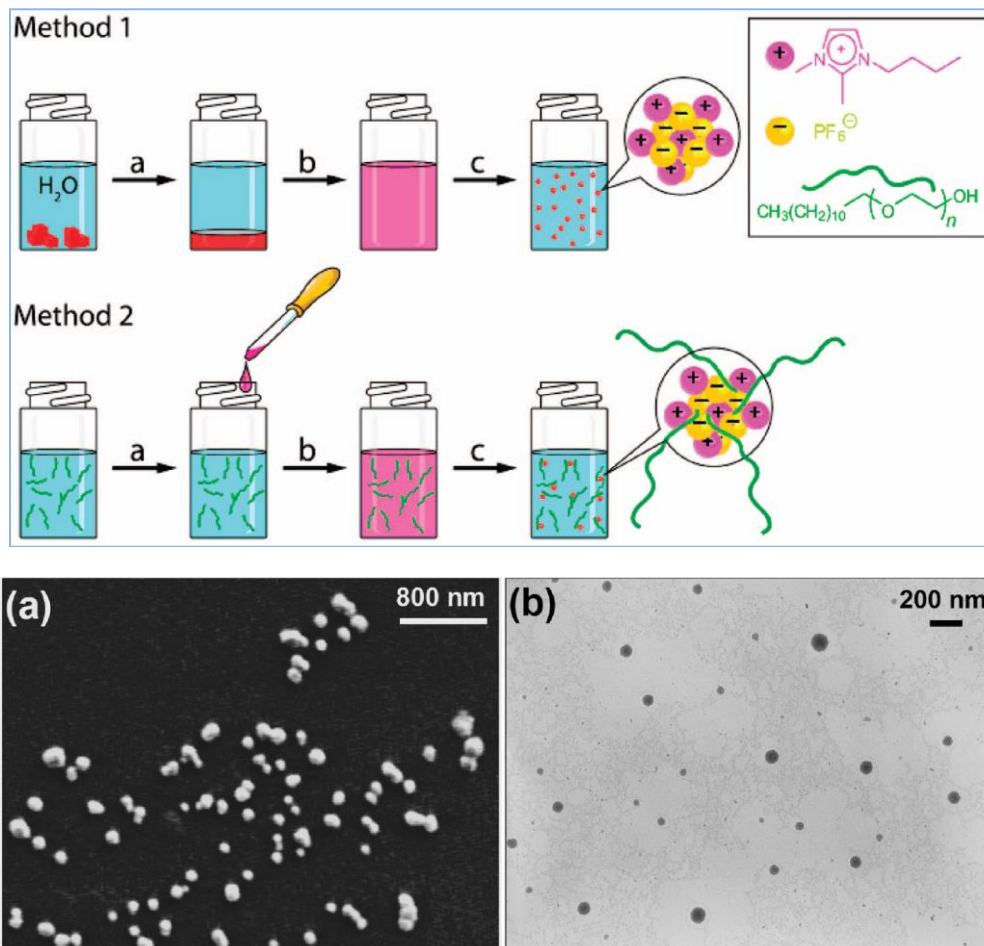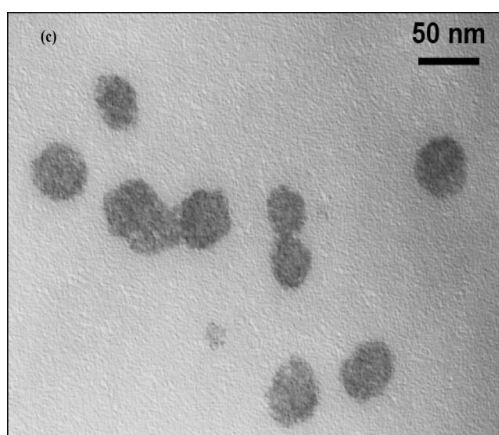
Figure 3. Scheme showing the Steps Involved in the Melt–Emulsion–Quench Method for the preparation of nano- and microparticles using surfactantless (Pathyway 1) and surfactant-assisted (Pathway 2) procedures. Electron micrographs of [bm2Im][PF$_6$] nanoparticles prepared using Pathway 1: (a) Scanning Electron Microscopy (SEM) image showing 90 nm on average diameter of nanoparticle; (b) Transmission Electron Microscopy (TEM) image showing 88 nm on average diameter of nanoparticle; (c) Transmission Electron Microscopy (TEM) image showing 45 nm on average diameter of nanoparticles prepared using Pathway 2 (using emulsifying agent- Brij35). Pictures taken from Nano Letts., 2008, Vol.8, 897-901. Published by: American Chemical Society.

Light Induced Synthesis: This methodology has been used commonly as a greener method to synthesize nanoparticles/ nanomaterials. As the name suggest, the technique involves light irradiation to pre-prepared materials and the light sources involved can be variable giving different controlled nano-dimension materials. Rehman *et al.* successfully biosynthesized silver nanoparticles using extracellular polymeric substances (EPS) from Chlamydomonas reinhardtii (a freshwater microalga), photon energy as the light induced source and obtained a three step mechanism for the reaction by establishing a relationship between EPS concentration, silver nanoparticles produced and photon input. The established mechanism claims to be helpful in the designing of photobioreactor (PBR) processes for nanoparticle production as well as its applicability in EPS-PBR-wastewater system [77]. 3 W LED diodes connected in a series (with same emission wavelength) as the light source have been used to prepare silver nanoparticles using DI (7 mL), aq. silver nitrate (0.01 M), aq. sodium benzoate (0.05 mL) (comparison with sodium salicylate, sodium citrate) and aq. PVP solution (1%) with addition of sodium borohydride (0.01 M). The process of irradiation has been done under refrigeration at a temperature maintained between 7 and 9 °C with excitation wavelengths of 455 nm of blue diodes and 595 nm of yellow diodes. SEM and AFM studies have shown aggregation of silver nanoparticles responsible for the particle plasma resonance. Such a light induced plasmon aggregation finds its potential in the synthesis of metallic nanoparticle clusters [78]. Researchers from Guanxi University, Nanning, southwest of China have reported the synthesis of silver-lignin nanoparticles using solar light irradiation as the light induced source. Lignin (16 mg) was dissolved in acetone (16 mL) with a dropwise (rate = 10 mL min^{-1}) subsequent addition of DI (64 mL, degassed with N$_2$, solvent) were magnetically stirred at 300 ± 20 rpm with lignin nanoparticles formed from self-assembly during the process. The prepared suspension was subjected to dialysis for 24 h in a dialysis bag (MWCO: 4000, Union carbide, Viskase, US) to assure complete removal of acetone which ultimately resulted in powdered LNPs under freeze drying for 24 h. They have experimented different concentration mixtures of LNPs suspensions and silver nitrate solutions for different times under solar irradiation using a glass vile as a reaction chamber and the reaction mixtures were passed under dialysis for removing Ag$^+$ particles giving Ag-LNPs suspensions which were stored in degassed DI in brown bottles under 4 °C. The frozen dried part of Ag-LNPs suspension studied using TEM, HRTEM, XRD and surface elemental analysis. Figure shows the pictures of TEM, HRTE and surface elemental techniques [79] (Figure 4).
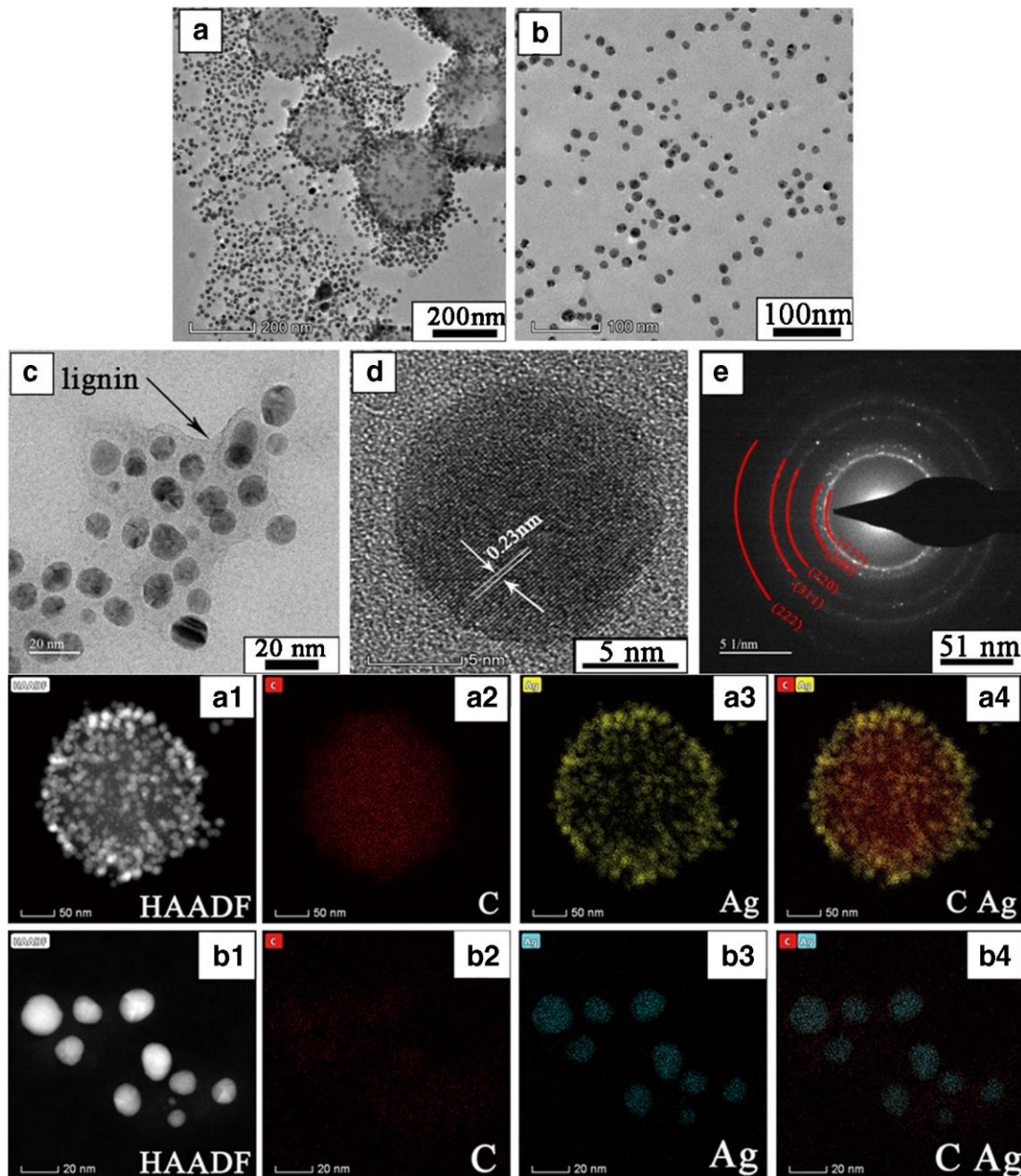
Figure 4 Transmission Electron Microscopy (TEM) images of Ag NP-LNP suspension (a), Ag NPs dissolved in water after centrifugation to remove LNPs (b). High Resolution Transmission Electron Microscopy (HRTEM) image of Ag NPs attached to lignin (c), image of individual silver nanoparticle (d), and Selected Area Electron Diffraction (SAED) of Ag NPs (e). High-Angle Annular Dark Field images (HAADF) and Element Mapping Analysis (EMA): Ag NPs loaded on LNPs (a1-a4) and Ag NPs entangled in lignin (b1-b4). Pictures taken from Michrochimica Acta (2019) 186:727 and Published by: Springer-Verlag GmbH Austria, part of Springer Nature 2019.

IV.   Summary and Outlook

To summarize, we say that nanocatalysis and naomaterial synthesis are totally interdependent and huge amount benefits to the both the areas will be observed if researchers are ready to chase this interdependence game with a positive oulook. In this pursuit of interdepndence, different nanomaterials have been explored and utilized like carbon naotubes, quantum dots, aerogels, titania based, ceria based nanomaterials, heteroatom doped nanomaterials and many more. Preparative techniques used for the synthesis of

nanomaterials serving other purposes like electrodes in batteries, in electronic devices, optical devices, sensor applications etc. can be applied to the synthesis of nanocatalysts and thus should be called as '*Nanocatalyst synthetic techniques with a twist*'. Sonme of these techniques that have been discussed include: molten salt emulsion methods, near field elecrospinning, nanoskiving, light induced, melt-emulsion method and high temperature heating methods. This concept of interdependence will help the researchers as well as the industry to grow by their efficient use in different spheres o finnovation and production. To support this, the review provides past as well as recent advancements in the experimental work. Moreover, such an interdependence will lower the consumption of time, energy and money. The content of discussion helps to sketch a future vision for a beneficial Interdependent NanoMatCat. generation.

Conflicts of interest
There is no conflict of interests.

References

[1]. E. G. Ewool, J. G. Davis, N. Ussiph, Int. J. Sci.Tech., 5 (2016), 396-415.
[2]. N. Srivastava, M. Srivastava, P. K. Mishra, M. A. Kausar, M. Saeed, V. K. Gupta, R. Singh, P. W. Ramteke, Biores. Tech., 307 (2020), 123094.
[3]. X. Liu, D. Huang, C. Lai, L. Qin, G. Zeng, P. Xu, B. Li, H. Yi, M. Zhang, Small (2019), 1900133-1900159.
[4]. F. Lu, D. Astruc, Coordination Chem. Rev., 408 (2020), 213180-213210.
[5]. X. Xu, X. Niu, X. Li, Z. Li, D. Du, Y. Lin, Sensors & Actuators: B. Chem., 315 (2020), 128100.
[6]. X. Y. Wong, A. S. Torralba, R. A. Diduk, K. Muthoosamy, A. Merkoci, ACS Nano, 14 (2020), 2585–2627.
[7]. L. Xu, J. Li, Y. Dong, J. Xue, Y. Gu, H. Zeng, Jizhong Song, ACS Appl. Mater. Interfaces, 11 (2019), 21100−21108.
[8]. S. Zhao, R. Nivetha, Y. Qiu, X. Guo, Chinese Chem. Letts., 31 (2020), 947-952.
[9]. D. Wang, D. Astruc, Chem. Soc. Rev., 46 (2017), 816-854.
[10]. M. Dhiman, V. Polshettiwar, Chem. Cat. Chem., 10 (2017), 881-906.
[11]. F. Li, Q. Tang, Phys. Chem. Chem. Phys., 21 (2019), 20144-20150.
[12]. Z. Guan, S. Lu, C. Li, J. Catal., 311 (2014), 1.
[13]. R. S. Ribeiro, A. M.T. Silva, P. B. Tavaresc, J. L. Figueiredo, J. L. Fariab, H. T. Gomes, Catal. Today, 249 (2015), 204-212.
[14]. S. Gunbatara, A. Aygunb, Y. Karatas, M. Gulcana, F. Sen, J. Colloid Interface Sci., 530 (2018), 321-327.
[15]. R. A. Rather, S. Siddiqui, W. A. Khan, Z. N. Siddiqui, Molecular Catalysis, 490 (2020), 110975.
[16]. H. Sohn, D. Kim, J. Lee, S. Yoon, RSC Adv., 6 (2016), 39484-39491.
[17]. Y. Chen, X. Li, X. Zhou, H. Yao, H. Huang, Y. W. Maiad, L. Zhou, Energy Environ. Sci., 7 (2014), 2689.
[18]. J. Wang, Z. Wei, Y. Gong, S. Wang, D. Su, C. Han, H. Li, Y. Wang, Chem. Commun., 51 (2015), 12859.
[19]. S. Verma, R. B. N. Baig, C. Han, M. N. Nadagoudab, R. S. Varma, Chem. Commun., 2015, 51, 15554-15557.
[20]. T. Chhabra, A. Bahuguna, S. S. Dhankhar, C. M. Nagaraja, V. Krishnan, Green Chem., 21 (2019), 6012.
[21]. Z. H. Yu, Y. L. Gan, J. Xu, B. Xue, Catal. Lett., 150 (2020), 301–311.
[22]. S. Ergen, B. Nisanci, O. Metin, New J. Chem., 42 (2018), 10000-10006.
[23]. N. D. Shcherban, P. Mäki-Arvela, A. Aho, S. A. Sergiienko, P. S. Yaremov, K. Eränen,
[24]. D. Yu. Murzin, Catal. Sci. Technol., 8 (2018), 2928-2937.
[25]. T. Hartman, Z. Sofer, ACS Nano, 13 (2019), 8566-8576.
[26]. K. Gopalakrishnan, A. Govindaraj, C.N.R. Rao, J. Mater.Chem. A, 1 (2013), 7563-7565.
[27]. Y. Zheng, H. Wang, S. Sun, G. Lu, H. Liu, M. Huang, J. Shi, W. Liu, H. Li, Sustain. Energy Fuels, 4 (2020), 1789-1800.
[28]. W. Ding, Z. Wei, S. Chen, X. Qi, T. Yang, J. Hu, D. Wang, L. J. Wan, S. F. Alvi, L. Li, Angew. Chem. Int. Ed., 52 (2013), 11755-11759.
[29]. J. Lilloja, E. K. Poldsepp, A. Sarapuu, A Kikas, V. Kisand, M. Kaarik, M. Merisalu, A. Treshchalov, J. Leisa, V. Sammelselg, Q. Weic, S. Holdcroft, K. Tammeveski, Appl. Catal. B: Environ., 272 (2020), 119012.
[30]. Z. S. Wu, W. Ren, L. Xu, F. Li, H.M. Cheng, ACS Nano, 5 (2011), 5463-5471.
[31]. D. Adekoya, H. Chen, H. Y. Hoh, T. Gould, M. S. Balogun, C. Lai, H. Zhao, S. Zhang, ACS Nano, 14 (2020), 5027-5035.

[32]. U. Maitra, U. Gupta, M. De, R. Datta, A. Govindaraj, C. N. R. Rao, Angew. Chem. Int. Ed., 52 (2013), 13057-13061.

[33]. S. L. Zhang, B. Y. Guan, X. W. D. Lou, Small, 15 (2019), 1970066.

[34]. W. Zhan, Y. Yuan, L. Sun, Y. Yuan, X. Han, Y. Zhao, Small, 15 (2019), 1901024.

[35]. C. N. R. Rao, K. Gopalakrishnan, A. Govindaraj, Nano Today, 9 (2014), 324-343.

[36]. R. A. Molla, Md. A. Iqubal, K. Ghosh, S. M. Islam, Green Chem., 18 (2016), 4649-4656.

[37]. S. Li, Q. Gu, N. Cao, Q. Jiang, C. Xu, C. Jiang, C. Chen, C. P. Huu, Y. Liu, J. Mater. Chem. A, 8 (2020), 8892-8902.

[38]. W. Yuan, J. Liu, W. Yi, L. Liang, Y. Zhu, X. Chen, J. Colloid Interf. Sci., 573 (2020) 232-240.

[39]. X. Liu, Y. Wan, L. Chen, P. Chen, S. Jia, Y. Zhang, S. Zhou, J. Zang, ACS Appl. Mater. Interfaces, 10 (2018), 37067-37078.

[40]. S. Ghosh, S. Ramaprabhu, J Colloid Interface Sci., 559 (2020), 169-177.

[41]. F. Brandi, M. Baumel, V. Molinari, I. Shekova, I. Lauermann, T. Heil, M. Antonietti, M. A. Naji, Green Chem., 22 (2020), 2755-2766.

[42]. 41. M. Siebels, C. Schlusener, J. Thomas, Y. X. Xiao, X. Y. Yang, C. Janiak, J. Mater. Chem. A, 7 (2019), 11934-11943.R.

[43]. 42. Saha, G. Sekar, Applied Catalysis B: Environmental, 250 (2019), 325–336.

[44]. 43. S. S. Mohire, G. D. Yadav, Ind. Eng. Chem. Res., 57 (2018), 9083-9093.

[45]. 44. F. Chen, B. Sahoo, C. Kreyenschulte, H. Lund, M. Zeng, L. He, K. Junge, M. Beller, Chem. Sci., 8 (2017), 6239-6246.

[46]. R. Baharfar, S. Mohajer, Catal. Lett., 146 (2016), 1729-1742.

[47]. Q. Liu, M. Luo, Z. Zhao, Q. Zhao, Chem. Eng., 380 (2020), 122423.

[48]. H. Veisi, T. Tamoradi, B. Karmakar, S. Hemmati, J. Phys. Chem. Solids, 138 (2020), 109256.

[49]. M. M. Aboelhassan, A. F. Peixoto, C. Freire, New J. Chem., 41 (2017), 3595-3605.

[50]. L. Kumar, S. Singh, A. Horechyy, P. Formanek, R. Hubner, V. Albrecht, J. Weibpflog, S. Schwarz, P. Puneeta, B. Nandan, RSC Adv., 10 (2020), 6592-6602.

[51]. B. C. Ledesma, J. M. Juarez, V. A. Valles, O. A. Anunziata, A. R. Beltramone, Catal. Lett., 147 (2017), 1029–1039.

[52]. M. Kour, M. Bhardwaj, H. Sharma, S. Paul, J. Clark, New J. Chem., 41 (2017), 5521-5532.

[53]. Y. S. Demidova, E. V. Suslov, O. A. Simakova, K. P. Volcho, N. F. Salakhutdinov, I. L. Simakova, D. Y. Murzin, J. Mol. Catal. A: Chem., 420 (2016), 142-148.

[54]. Y. Yang, N. Liu, S. Qiao, R. Liu, H. Huang, Y. Liu, New J. Chem., 39 (2015), 2815-2821.

[55]. M. Mohammadi, A. Khazaei, A. Rezaei, Z. Huajun, S. Xuwei, ACS Sustainable Chem. Eng., 7 (2019), 5283-5291.

[56]. X. Li, X. Jiang, Q. Liu, A. Liang, Z. Jiang, Nanomaterials, 9 (2019), 223.

[57]. Z. S. Mahmoudabadi, A. Rashidi, A. Tavasoli, J. Environ. Chem. Engg., 8 (2020), 103736.

[58]. R. M. Tesfaye, G. Das, B. J. Park, J. Kim, H. H. Yoon, Scientific Reports, 9 (2019), 479.

[59]. X. Yang, J. Wei, Q. Wang, M. Shuai, G. Yue, P. Li, D. Huang, D. Astruc, P. Zhao, Nanoscale, 12 (2020), 2345-2349.

[60]. L. Minati, K. A. Zinsou, V. Micheli, G. Speranza, Dalton Trans., 47 (2018), 14573-14579.

[61]. P. A. R. Pereira, D. A. Ceccato, A. G. B. Junior, M. F. S. Teixeira, S. A. M. Lima, A. M. Pires, RSC Adv., 6 (2016), 104529-104536.

[62]. G. Kour, M. Gupta, Dalton Trans., 46 (2017), 7039-7050.

[63]. Y. Mao, X. Yang, W. Gong, J. Zhang, T. Pan, H. Sun, Z. Chen, Z. Wang, J. Zhu, J. Hu, S. Cong, F. Geng, Z. Zhao, Small, 16 (2020), 2001098.

[64]. S. He, H. Du, K. Wang, Q. Liu, J. Sun, Y. Liu, Z. Du, L. Xie, W. Ai, W. Huang, Chem. Commun., 56 (2020), 5548-5551.

[65]. C. Wang, Y. Chen, T. Hu, Y. Chang, G. Ran, M. Wang, Q. Song, Nanoscale, 11 (2019), 11967-11974.

[66]. A. Shavel, L. Guerrini, R.A. A. Puebla, Nanoscale, 9 (2017), **9**, 8157-8163.

[67]. D. Sun, C. Chang, S. Li, L. Lin, Nano Lett., 6 (2006), 839-842.

[68]. Y. S. Park, J. Kim, J. M. Oh, S. Park, S. Cho, H. Ko, Y. K. Cho, Nano Lett., 20 (2020), 441–448.

[69]. J. Zheng, B. Sun, X. X. Wang, Z. X. Cai, X. Ning, S. M. Alshehri, T. Ahamad, X. T. Xu, Y. Yamauchi, Y. Z. Long, Polymers, 12 (2020), 695.

[70]. Q. Xu, R. M. Rioux, M. D. Dickey, G. M. Whitesides, Acc Chem. Res., 41 (2008), 1566-1577.

[71]. Z. Fang, Y. Geng, J. Wang, Y. Yan, G. Zhang, **Nanoscale**, 12 (2020), 8194-8199.

[72]. P. Gu, Z. Zhou, Z. Zhao, H. Mohwald, C. Li, R. C. Chiechi, Z. Shi, G. Zhang, Nanoscale, 11 (2019), 3583-3590.

[73]. M. Xu, Y. Zhang, K. Wang, J. Mao, W. Ji, W. Qiu, T. Feng, M. Zhang, L. Mao, Analyst, 144 (2019), 2914-2921.

[74]. L. Jibril, J. Ramirez, A. V. Zaretski, D. J. Lipomi, Sens. Actuator Phys. A, 263 (2017), 702–706.

[75]. A. Tesfai, B. E. Zahab, D. K. Bwambok, G. A. Baker, S. O. Fakayode, M. Lowry, I. M. Warner, Nano Lett., 8 (2008), 897-901.

[76]. M. R. Ahmed, A. V. L. Phani, M. N. Chary, Md.Shareefuddin, AIP Conference Proceedings 1953, 090037 (2018); DOI: 10.1063/1.5032884. Published by American Institute of Physics.

[77]. N. Shukla, D. K. Dwivedi, J. Asian Ceram. Soc., 4 (2016), 4, 178-184.

[78]. A. Rahman, S. Kumar, A. Bafana, J. Lin, S. A. Dahoumane, C. J. Ryes, Molecules, 24 (2019), 3506.

[79]. A. I. Tolpintseva, O. Tynkevych, A. Diaconu, A. Rotaru, Y. Khalavka, Appl. Nanosci., 9 (2018), 709-714.

[80]. Q. Zhang, C. Chen, G. Wan, M. Lei, M. Chi, S. Wang, D. Min, Microchim. Acta., 186 (2019), 727.